



Published in final edited form as:

Cancer Chemother Pharmacol. 2011 July ; 68(1): 17–27. doi:10.1007/s00280-010-1440-8.

Cryptotanshinone has diverse effects on cell cycle events in melanoma cell lines with different metastatic capacity

Lei Chen,

Department of Clinical Pharmacy, School of Pharmacy, Nanjing University of Chinese Medicine, 282 Hanzhong Road, 210029 Nanjing, Jiangsu, People's Republic of China

Shi-zhong Zheng,

Department of Clinical Pharmacy, School of Pharmacy, Nanjing University of Chinese Medicine, 282 Hanzhong Road, 210029 Nanjing, Jiangsu, People's Republic of China

Zhi-guang Sun,

Department of Clinical Pharmacy, School of Pharmacy, Nanjing University of Chinese Medicine, 282 Hanzhong Road, 210029 Nanjing, Jiangsu, People's Republic of China

Ai-yun Wang,

Department of Clinical Pharmacy, School of Pharmacy, Nanjing University of Chinese Medicine, 282 Hanzhong Road, 210029 Nanjing, Jiangsu, People's Republic of China

Chen-hu Huang,

Department of Clinical Pharmacy, School of Pharmacy, Nanjing University of Chinese Medicine, 282 Hanzhong Road, 210029 Nanjing, Jiangsu, People's Republic of China

Neville A. Punchard,

School of Health and Bioscience, University of East London, London E15 4LZ, UK

Shi-le Huang,

Department of Biochemistry and Molecular Biology, Feist-Weiller Cancer Center, Louisiana State University Health Sciences Center, New Orleans, LA 71130-3932, USA

Xiang Gao, and

Model Animal Research Center, Nanjing University, 12 Xuefu Road, Pukou District, 210061 Nanjing, Jiangsu, People's Republic of China

Yin Lu

Department of Clinical Pharmacy, School of Pharmacy, Nanjing University of Chinese Medicine, 282 Hanzhong Road, 210029 Nanjing, Jiangsu, People's Republic of China

Jiangsu Key Laboratory for Traditional Chinese Medicine Formulae Research, Nanjing University of Chinese Medicine, 210046 Nanjing, People's Republic of China

Xiang Gao: gaoxiang@nju.edu.cn; Yin Lu: luyingreen@126.com

Abstract

Purpose—Cryptotanshinone is a major active component of *Salvia miltiorrhiza*, which is often used as Chinese herbal medicine in cancer therapy. Here, we systematically assessed the anti-

© Springer-Verlag 2010

Correspondence to: Yin Lu, luyingreen@126.com.

Electronic supplementary material The online version of this article (doi:10.1007/s00280-010-1440-8) contains supplementary material, which is available to authorized users.

tumor effect of Cryptotanshinone on two melanoma cell lines with low/high-metastatic capacity (B16/B16BL6).

Methods—MTT and LDH assays were used to evaluate cell growth and cytotoxicity. We assessed the effect of Cryptotanshinone on cell apoptosis or proliferation by Annexin V, TUNEL or BrdU assay. Cell cycle distribution was detected by flow cytometry. The integrity of cell cycle checkpoints was determined by mutational analyses of B-RAF and N-RAS, and the expression of cell cycle-associated proteins by western blotting.

Results—Treatment with Cryptotanshinone had no obvious effect on cell apoptosis but significantly inhibited cell proliferation. Cryptotanshinone slightly increased the expression of p53, Chk1, and Chk2 in both B16 and B16BL6. Interestingly, Cryptotanshinone induced G1 arrest with a concomitant increase in p21 expression in B16BL6 cells. However, in B16 cells, Cryptotanshinone induced the G2/M arrest through its induction of Cdc25c. Regulation of Cyclin A1, Cyclin B1 and Cdk1/cdc2 expression might contribute to the different cell cycle patterns in B16 and B16BL6 after Cryptotanshinone treatment.

Conclusions—Cryptotanshinone could have diverse effects on cell cycle events in melanoma cell lines with different metastatic capacity. This property might offer an opportunity to study underlying mechanisms for the different antitumor effects of administered Cryptotanshinone in B16 and B16BL6 cells.

Keywords

Cryptotanshinone; Cell cycle arrest; Melanoma; B16; B16BL6

Introduction

Melanoma is a form of cancer that arises from melanocytes, specialized pigmented cells that are found predominantly in the skin [1]. The incidence of melanoma in many countries has risen by 3–8% per year since the mid-1960s [2,3], and in Western populations, the number of cases has doubled in the past 20 years [1]. It is an extremely aggressive disease with high-metastatic potential and a notoriously high frequency of drug resistance. Melanomagenesis is relevant to defects in nucleotide excision repair of DNA damage induced by solar radiation. After DNA damage and oncogene activation, cell cycle checkpoints arrest cell growth [4].

Identification of new drugs from plants has a long and successful history [5]. *Salvia miltiorrhiza* (Danshen), a well-known traditional Chinese herbal medicine, is widely used in the clinical treatment of different diseases [6–9]. In the Dictionary of Traditional Chinese Medicine Prescription, Danshen came in fourth place among 1362 anticancer classic and empirical prescription by frequency analysis. Therefore, Danshen play an important role in traditional Chinese medicine for cancer treatment. Chemical constituents of this medicine have been investigated since 1934. Along with more than 20 phenolic acids, about 30 diterpene compounds have been isolated from Danshen, including the relatively abundant tanshinones, such as tanshinone I, tanshinone IIA, Cryptotanshinone and dihydrotanshinone [7]. Cryptotanshinone (Fig. 1), as a major active component, has been shown to possess pharmacological activities, such as anticholinesterase, anti-inflammatory, antioxidative, antibacterial, antitumor and antiplatelet aggregation [10–15]. Recent studies have also shown that Cryptotanshinone is a potential anticancer agent [16,17]. However, the anticancer mechanism of Cryptotanshinone remains to be elucidated.

Tumorigenesis encompasses multiple processes involved in the dysregulation of a number of molecular pathways, such as cell cycle, proliferation and apoptosis. The strategy behind

some forms of drug therapy is to either retard cell cycle progression or induce apoptosis. The aim of this study was to investigate the possible roles of Cryptotanshinone on melanoma cell lines with different metastatic capacity, including the high-metastatic potential melanoma cell line (B16BL6) and the low-metastatic potential melanoma cell line (B16). The use of pairs of cell lines, one with a very low and the other with a very high capacity to metastasize, offers an opportunity to dissect out the various processes involved.

Materials and methods

Animals

Female C57BL/6 mice (6–8 weeks old) were purchased from the Slac Animal Inc (Shanghai, China). Throughout the experiments, mice were maintained in plastic cages at $21 \pm 2^\circ\text{C}$, on a 12-h light/dark cycle and with free access to food and water. Animal welfare and experimental procedures were performed strictly in accordance with the care and use of laboratory animals and the related ethics regulations of our University. All possible efforts were made to minimize the animals' suffering and to reduce the number of animals used.

Cell lines and culture condition

These studies utilized C57BL/6 mice-derived melanoma cell lines, including B16 (low-metastatic potential) and B16BL6 (high-metastatic potential), which were kindly provided by Nanjing University. The cells were cultured as a monolayer in DMEM (Gibco, Grand Island, NY, USA), containing 10% v/v fetal bovine serum (Hyclone, Canada), penicillin (100 IU/ml), streptomycin (100 $\mu\text{g/ml}$) and 3.7 mg/ml NaHCO_3 . All cells were grown in a humidified atmosphere, containing 5% CO_2 at 37°C .

Experimental metastasis model

The suspension of B16 or B16BL6 cells (5×10^5 cells in 0.2 ml per mouse) was injected through the tail vein of a 6- to 8-week-old female C57BL/6 J mice and allowed to locate to the lungs, where they extravasated into the lung parenchyma. All mice were killed 23 days after the injection of the tumor cells. The lungs were then removed, weighed and fixed. The metastatic foci on the surfaces of the lung were photographed and counted.

MTT assay

In this study, 100 mM stock solution of Cryptotanshinone (Xi'an Helin Biological Engineering Co., Ltd. Xi'an, China, purity >95%) was prepared in ethanol, then filtered by 0.2- μm membrane and diluted as indicated. Solvent control was also prepared for the treatment of cultures. The growth inhibition effect of Cryptotanshinone on melanoma cells was carried out using the MTT assay. Briefly, exponentially growing cells, seeded in 96-well plates (5×10^3 cells/well), were incubated in the presence of different concentrations (0.1–100 μM) of Cryptotanshinone for different periods of time. At the end of the incubation period, 20 μl of a stock solution of 5 mg/ml 3-(4,5)-dimethylthiazolium (-z-y1)-3,5-diphenyltetrazolium bromide (MTT; Amresco, USA) was added to each well, and plates were gently shaken and incubated at 37°C . After a further 4-h incubation, the cells were lysed with dimethyl sulfoxide and quantified at OD_{490} using an enzyme-linked immunosorbent assay reader.

Cell morphological analysis

Cells were seeded at a density of 2×10^5 cells/well in a 6-well plate and grown overnight. The next day, different concentrations of Cryptotanshinone were added (final concentration of 0, 1, 10 and 25 μM). After incubation for 24 h, images of the cell morphological changes

were taken with an inverted microscope at a 100× magnification by a Leica Qwin system (Leica, LEITZ WETZLAR, Germany).

LDH assay

Cytotoxicity was determined by measuring cell membrane damage through the release of lactate dehydrogenase (LDH). For this experiment, exponentially growing cells were seeded in 96-well plates (5×10^3 cells/well) and incubated for 24 h in complete medium. The cells were then incubated in the presence of varying concentrations of Cryptotanshinone as indicated for 24 h. Culture supernatants were then collected from each well, and the LDH release assay was performed according to the manufacturer's instructions. The LDH kit was purchased from the Nanjing Jiancheng Bioengineering Institute (Nanjing, China).

Annexin V assay [6]

Cells, seeded in 6-well plates at a density of 2×10^5 cells/well in growth medium, were grown overnight at 37°C in a humidified incubator with 5% CO₂. Cells were then treated with Cryptotanshinone (0, 1, 10 and 25 μM) for 24 h. Cell apoptosis was assessed by Annexin V-FITC staining using a flow cytometric apoptosis detection kit (Cat.No. 556420, BD Biosciences Pharmingen, San Jose, CA). The stained cells with Annexin V-FITC/propidium iodide were analyzed using a BD FACSCalibur™ flow cytometer and CellQuest analysis software (BD Biosciences, Mountain View, CA).

TUNEL assay

Cells (2×10^5 cells/well) were seeded in growth medium on Poly-L-Lysine (P4707, Sigma)-coated cover glass slides in 6-well plates and grown overnight at 37°C, in a humidified incubator with 5% CO₂. Cells were then treated with Cryptotanshinone (0, 1, 10 and 25 μM) for 24 h. After that, cells were examined for apoptosis by terminal deoxynucleotidyl transferase-mediated dUTP nick-end labeling (TUNEL) assay (Promega, Madison, WI), performed according to the manufacturer's instructions as previously described [18]. Cells were visualized and photographed using Leica TCS-SL confocal system (Leica Microsystems, Mannheim, Germany). At least five randomly chosen areas in every slide were used.

BrdU assay

Cells (2×10^5 cells/well) were seeded in growth medium on Poly-L-Lysine-coated cover glass slides in 6-well plates and grown overnight at 37°C in a humidified incubator, with 5% CO₂. Cells were then treated with Cryptotanshinone (0, 1, 10 and 25 μM) for 24 h. After that, cells were incubated with 5-bromo-2-deoxyuridine (BrdU; B5002, Sigma) at a final concentration of 10 μM for 30 min at 37°C. The slides were washed with cold PBS prior to fixing with 4% PFA for 10 min. Subsequently, slides were washed with PBS and incubated with 2 N HCl for 25 min. After washing with PBS and incubating with blocking buffer (2.5% bovine serum albumin, 1% normal goat serum and 0.5% Tween 20 in PBS), the slides were incubated with mouse anti-BrdU antibody (1:100, Roche) at 37°C for 2 h. The slides were then washed with PBS and incubated with FITC-labeled goat anti-mouse IgG (1:200, Sigma) for 1 h at room temperature. After washing again, the slides were incubated with Topro-3 (1:300, Invitrogen) in PBS for 15 min to counterstain the nuclei and mounted on slides using 50% glycerol. Cells were visualized and photographed using Leica TCS-SL confocal system. At least five randomly chosen areas in every slide were taken.

Cell cycle assay

Cells were seeded in growth medium in 60-mm dishes at a density of 3×10^5 cells/dish and were grown overnight at 37°C, in a humidified incubator with 5% CO₂. Cells were then

treated with Cryptotanshinone (0, 1, 10 and 25 μM) for 6, 12, 24 and 48 h. The population at each stage of the cell cycle was analyzed by flow cytometry. Briefly, cells were trypsinized, washed twice with PBS and fixed in 70% ethanol overnight at -20°C . Fixed cells were then washed with PBS, incubated with 0.5 ml PBS containing 100 $\mu\text{g}/\text{ml}$ RNase and stained with 40 $\mu\text{g}/\text{ml}$ propidium iodide for 30 min at 37°C . The stained cells were analyzed using a BD FACSCalibur™ flow cytometer and CellQuest analysis software (BD Biosciences, Mountain View, CA).

Mutational analyses of B-RAF and N-RAS

The N-RAS and B-RAF mutational status was determined from genomic DNA for the melanoma cell lines (B16 and B16BL6). Genomic DNA was isolated from cells, and the mutational status of N-RAS at exons 1 and 2 and B-RAF at exons 14 and 18 were determined as follows: PCR amplification utilized the following primers [19], then PCR products were purified from 1% agarose gels and DNA was sequenced using the forward PCR primers at GenScript Corporation (Nanjing, China).

N-RAS at exon 1 forward: 5'-TTGCTGCTTTTCTACAG G-3',

reverse: 5'-CCAAAGTGAGGATAAGGG-3';

N-RAS at exon 2 forward: 5'-CCTCCTCACTCTTTCATATTCC-3',

reverse: 5'CAGAAAATATCCCCAGTACC-3'

B-RAF at exon 14 forward: 5'GGCAGGTCAATATAGTTAGC-3',

reverse: 5'-CGTGTTATACATACCATGTCC-3';

B-RAF at exon 18 forward: 5'-CAAATGCTTTCTCTAATAGG-3',

reverse: 5'-TAAGCAGTCACTAGTTTAGG-3'

Western blotting assay

To detect the effects on cell cycle-associated protein expression in B16 and B16BL6 cells, cells seeded in 6-well plates at a density of 2×10^5 cells/well in growth medium were grown overnight at 37°C in a humidified incubator with 5% CO_2 . Cells in culture were then treated with different concentrations of Cryptotanshinone or media only (control) for 24 h. After that, cells were washed with pre-cooled PBS and lysed in radioimmunoprecipitation assay (RIPA) buffer supplemented with 1 mM PMSF, 1 mM Na_3VO_4 , 1 mM NaF and 1:100 dilution of Protease Inhibitor Cocktail (Sigma, St. Louis, MO, USA). Protein samples were resolved by SDS-PAGE and transferred to a polyvinylidene difluoride membrane (Millipore, Billerica, MA). p53, checkpoint kinase 1 (Chk1), checkpoint kinase 2 (Chk2), p21, Cyclin A1, Cyclin B1, cyclin-dependent kinase 1/cell division cycle 2 (Cdk1/Cdc2) and cell division cycle 25 homolog C (Cdc25c) proteins were detected by immunoblot with anti-p53 (1:500, NCL-p53-CM5p, Novocastra, Newcastle, UK), anti-Chk1 (1:200, BS1053, Bioworld Technology, Bioworld, USA), anti-Chk2 (1:200, BS1391, Bioworld Technology, Bioworld, USA), anti-p21 (1:200, sc-6246, Santa Cruz Biotechnology, Santa Cruz, CA), anti-Cyclin A1 (1:200, BS1804, Bioworld Technology, Bioworld, USA), anti-Cyclin B1 (1:200, sc-752, Santa Cruz Biotechnology, Santa Cruz, CA), anti-Cdk1/Cdc2 (1:200, BS1820, Bioworld Technology, Bioworld, USA), anti-Cdc25c (1:200, sc-327, Santa Cruz Biotechnology, Santa Cruz, CA), polyclonal antibody and β -actin (1:15000; Sigma St Louis, MO, USA) or GAPDH (1:5000, sc-32233, Santa Cruz Biotechnology, Santa Cruz, CA), then followed by incubation with peroxidase-coupled secondary antibodies. A Supersignal kit (Pierce, Rockford, IL) was used to visualize the bands according to the manufacturer's instructions.

Statistical analysis

The data obtained from at least three independent tests are presented as means \pm S.E.M., and statistical comparisons between groups were performed using one-way ANOVA followed by Student's *t*-test at *P* values of <0.001 (***), <0.01 (**) or <0.05 (*).

Results

Effect of Cryptotanshinone on B16 and B16BL6 melanoma cell growth

The possible roles of Cryptotanshinone on melanoma cell lines with different metastatic capacities were investigated. First of all, we established an *in vivo* experimental metastasis model to confirm the exact metastatic capacity of B16 (low-metastatic potential) and B16BL6 (high-metastatic potential) melanoma cell lines. Compared with the B16 melanoma cell group, B16BL6 melanoma cells remarkably increased the lung weight and the number of tumor nodules on the lung surface in the experimental metastasis model (Supplementary Fig. 1). Next, we tested the effect of Cryptotanshinone on cell growth of B16 and B16BL6 melanoma cell lines *in vitro* by the MTT assay. As shown in Fig. 2A, Cryptotanshinone caused a strong concentration-dependent inhibition in B16 and B16BL6 melanoma cell growth. The half-maximal inhibitory concentration (IC₅₀) of Cryptotanshinone on B16 and B16BL6 cells was 12.37 and 8.65 μ M, respectively. Cells were then treated with various concentrations of Cryptotanshinone (0, 1, 10 and 25 μ M) at different time periods (4, 8, 12, 16, 20 and 24 h), and the MTT assay was performed at the end of each treatment. A marked reduction in viable cell count was observed after treatment with Cryptotanshinone in both a time- and dose-dependent manner (Fig. 2B). At the same time, the cell viability following Cryptotanshinone treatment was further confirmed by morphological analyses. The present results demonstrated that Cryptotanshinone was able to inhibit cell growth and induce morphological changes (Fig. 2C). The cytotoxic effect of Cryptotanshinone on B16 and B16BL6 cells was also determined using the LDH assay (Fig. 2D). We found that cytotoxic effect triggered by Cryptotanshinone occurred at concentrations above 25 μ M, with significant effects seen at 50–100 μ M and that there was no significant adverse effect of Cryptotanshinone at lower (0–25 μ M) concentrations. These results indicated that the growth inhibition of Cryptotanshinone (0–25 μ M) was due to cytostatic rather than cytotoxic effect.

Effect of Cryptotanshinone on B16 and B16BL6 melanoma cell apoptosis

To determine whether the growth inhibitory effect of Cryptotanshinone was associated with the induction of apoptosis, B16 and B16BL6 cells were exposed to Cryptotanshinone (0, 1, 10 and 25 μ M) for 24 h. After that, these cells were stained with annexin V-FITC/propidium iodide (PI) and then determined by flow cytometry. As shown in Fig. 3A, Cryptotanshinone increased the percentage of apoptotic cells in a concentration-dependent manner, but the effect was slight. At 25 μ M, Cryptotanshinone only induced apoptosis in approximately 4% of cells. Similar results were obtained in B16BL6 cells, suggesting that the effect of Cryptotanshinone on apoptosis in both B16 and B16BL6 melanoma cells was of lesser relevance, and the change may have no biological meaning. FITC-linked Annexin V/propidium iodide staining assay provides a simple and effective method to detect apoptosis at a very early stage, while terminal deoxynucleotidyl transferase dUTP nick end labeling (TUNEL) is a method for identifying cells in the last phase of apoptosis. To further strengthen the evidence, TUNEL assay was used to confirm the effect of Cryptotanshinone on apoptosis, and confirmatory results were obtained by TUNEL staining through counting the apoptotic cells (Fig. 3B).

Effect of Cryptotanshinone on B16 and B16BL6 melanoma cell proliferation (DNA synthesis)

Cell proliferation and apoptosis are intimately linked, thus the coordination, and balance, between these two processes is crucial for normal cell physiology. When the cell enters the S phase (DNA synthesis), the cellular DNA is duplicated. Cells in S phase were labeled by BrdU incorporation, assayed by immunostaining and counted using confocal microscopy. Cryptotanshinone treatment resulted in a decreased number of BrdU-positive cells in a dose-dependent manner (Fig. 4), indicating that the percentage of cells in the S phase, and hence undergoing DNA synthesis, was reduced.

Effect of Cryptotanshinone on B16 and B16BL6 melanoma cell cycle

The cell cycle is a critical regulator of the processes involved in cell proliferation and growth, as well as cell division after DNA damage. To explore whether the observed growth inhibitory effect of Cryptotanshinone was caused by specifically perturbing cell cycle-related events, a set of experiments were performed to measure both DNA content and the cell cycle distribution of Cryptotanshinone-treated, or untreated, cells by flow cytometry after staining with PI. As shown in Fig. 5, the population of cells in the S phase continuously decreased both in B16 and B16BL6 cells in a concentration- and time-dependent manner after exposure to Cryptotanshinone, consistent with the results of the BrdU assay. At the same time, the sub-G1 peak (apoptosis peak) was not observable, which was consistent with the findings of Annexin V and TUNEL assay. Interestingly, the data indicated that during the 48-h time period, treatment of B16 and B16BL6 cells with Cryptotanshinone led to a marked accumulation of cells in the G2 phase and G1 phase, respectively. Such effects were not observed in control cells. The Cryptotanshinone-treated cells (25 μ M) showed the typical patterns of DNA content that arrested at G2/M phase in B16 cells (Fig. 5B a) and blocked at G1 phase in B16BL6 cells (Fig. 5B b), respectively.

Mutational analyses of B-RAF and N-RAS in B16 and B16BL6 cell lines

Defects in DNA damage responses may result in genetic instability and malignant progression in melanoma. A majority of melanoma cell lines display significant quantitative defects in one or both checkpoints. For example, Kaufmann et al. [4] found that the epithelial-like subtype of melanomas with wild-type N-RAS and B-RAF alleles show an effective G2 checkpoint, but a significant defect in G1 checkpoint function. In contrast, melanomas with B-RAF mutations display a significant defect in G2 checkpoints. In the current experiments, flow cytometry indicated that Cryptotanshinone induced G1 arrest in B16BL6 and G2 arrest in B16. The question was ‘Why did Cryptotanshinone have diverse effects on cell cycle events in these two cell lines?’ We hypothesized that high-metastatic (B16BL6) and low-metastatic (B16) potential melanoma cell lines could display different defects in cell cycle checkpoint functions, in order for cells to proliferate with the chromosomal instability that characterizes this malignancy. We thus analyzed genomic DNA from B16 and B16BL6 melanoma cell lines for oncogenic mutations in N-RAS and B-RAF. However, sequencing of the PCR products did not reveal any mutations in these two cell lines (data not shown).

Effect of Cryptotanshinone on the expression of cell cycle-associated proteins in B16 and B16BL6 melanoma cells

Cell cycle progression is regulated by checkpoint controls, which function to protect genome integrity and prevent cell cycle progression until after completion of prior events [20]. The G1 checkpoint permits repair of the genome prior to its replication, while G2 checkpoint permits repair prior to mitotic separation. The tumor suppressor p53 primarily controls G1 arrest. Both Chk 1 and Chk 2 function as essential components in the G2 DNA damage

checkpoint by phosphorylating Cdc25c in response to DNA damage [21]. Therefore, we speculated that the different cell cycle events induced by Cryptotanshinone in B16 and B16BL6 cells was correlated with the induction of different checkpoint-associated proteins. Our western blotting analysis showed that the expression of p53, Chk1 and Chk2 was slightly increased in B16 and B16BL6 cells at 24 h following treatment with Cryptotanshinone (Fig. 6a), though the degree of the increase and the basal expression of p53, Chk1 and Chk2 were slightly different in B16 when compared to B16BL6 cells. To further understand the molecular mechanisms involved, we next investigated the effects of Cryptotanshinone on the cyclin-dependent kinase (Cdk) inhibitor, p21 [22], which mediates p53-dependent G1 growth arrest. Incubation of B16BL6 cells with Cryptotanshinone, which arrested at G1 phase, caused a dose-dependent increase in p21 protein level. On the other hand, Cryptotanshinone treatment of B16 cells, which led to a cell cycle arrest at G2 phase in these cells, had no obvious effect on the protein level of p21 (Fig. 6b). In addition, Cdc25, which dephosphorylates and activates Cdks, is one of the major and crucial targets for Chk1 and Chk2 in cell cycle checkpoints [23,24]. We found that the level of Cdc25c was increased in B16, but decreased in B16BL6, cells in response to Cryptotanshinone treatment (Fig. 6b). In mammalian cells, progression through the G2 phase of the cell cycle is mediated by a specific set of proteins, which include Cyclins A1, B1 and mitotic kinase Cdk1 (alias p34Cdc2) [25]. After Cryptotanshinone treatment, B16 cells in the G2/M phase expressed Cyclin A1, Cyclin B1 and Cdk1/cdc2 at a higher level, while B16BL6 cells in the G1 phase expressed these regulatory proteins at a lower level (Fig. 6c).

Discussion

Melanoma is characterized by high-metastatic propensity, infamous cancer therapy resistance and extremely poor patient survival rate. It is the second most rapidly growing type of cancer in humans [26]. In this study, the results showed that Cryptotanshinone was a potent inhibitor of B16 and B16BL6 melanoma cell growth. The balance of cell progression is a series of tightly integrated events that allows cells to grow, proliferate and undergo apoptosis. However, we could not detect any obvious apoptosis in Cryptotanshinone-treated cells. Subsequent experiments addressed whether Cryptotanshinone inhibited cell proliferation, as measured by the BrdU assay. The data for Cryptotanshinone-treated cells clearly revealed a significant reduction of the S phase in cells. To confirm that the effect induced by Cryptotanshinone was associated with the arrest of cells in a particular phase, we analyzed cell distribution at each phase of the cell cycle by flow cytometry. We found that Cryptotanshinone inhibited the cell proliferation by inducing the G2/M arrest in a dose-dependent manner in the B16 cell line. This observation was different from the results obtained from the B16BL6 cell line, which showed an increased cell population in the G1 phase. Analyses for B-RAF and N-RAS in B16 and B16BL6 cell lines did not reveal any mutations. We supposed the reason for this difference in behavior induced by Cryptotanshinone might be due to the different modulation of cell cycle-regulatory proteins rather than the different defects in cell cycle checkpoint function in these two melanoma cell lines. We found that Cryptotanshinone induced G1 arrest with a concomitant increase in p21 expression in B16BL6 cells. However, in B16 cells, Cryptotanshinone induced the G2/M arrest through its induction of Cdc25c. Regulation of Cyclin A1, Cyclin B1 and Cdk1/cdc2 expression might contribute to the different cell cycle patterns in B16 and B16BL6 after Cryptotanshinone treatment.

Cryptotanshinone was shown to arrest B16BL6 cells in G1 and block B16 cells at the G2/M transition. The reason for this difference in behavior induced by Cryptotanshinone in these two cell lines might be due to their distinct properties of these two cell lines. Similar conflicting results have been presented in other reports. For example, Casagrande et al. [27] has summarized that quercetin could block the cell cycle at the G1/S transition in colon and

gastric cancer cells as well as in leukemic cells. Meanwhile, quercetin has also been found to cause a G2/M arrest in breast and laryngeal cancer cell lines, and in non-oncogenic fibroblasts. Similarly, some reports have indicated that As₂O₃ induced cell cycle arrest at either G1 or G2/M phase also depending on the cell line used [28].

The results also revealed differences in structure–activity relationship between the tanshinones. Mosaddik et al. [29] has studied the cytotoxic effect of four tanshinones isolated from *Salvia miltiorrhiza Bunge* on P388 lymphocytic leukemia cells and suggested that the critical structural components for the cytotoxicity of these diterpenes may depend on unsaturated C-15 and saturated ring A. This result was consistent with our evidence in that Cryptotanshinone, which lacks unsaturation at C-15, showed little cytotoxicity, but possessed a potent cytostatic effect. Therefore, due to this lack of cytotoxic effect, Cryptotanshinone may have potential as a lead compound in the development of chemotherapeutic agents. While the antiproliferative effect of Cryptotanshinone represents a potential cancer chemopreventive mechanism, the cell cycle effect of Cryptotanshinone in vivo also requires further study. Furthermore, Cryptotanshinone, which appears to have diverse effects on cell cycle events in melanoma cell lines with different metastatic capacity, offers a useful tool to investigate the reasons behind such different patterns of malignancy.

Supplementary Material

Refer to Web version on PubMed Central for supplementary material.

Abbreviations

DMEM	Dulbecco's modified Eagle medium
MTT	3-(4,5)-dimethylthiazoliazol(-z-y1)-3,5-diphenyltetrazoliumromide
IC50	Half-maximal inhibitory concentration
LDH	Lactate dehydrogenase
TUNEL	Terminal deoxynucleotidyl transferase-mediated dUTP nick-end labeling
BrdU	5-bromo-2-deoxyuridine
NHMs	Normal human melanocytes
RIPA	Radioimmunoprecipitation Assay
Chk1	Checkpoint kinase 1
Chk2	Checkpoint kinase 2
Cdk1/cdc2	Cyclin-dependent kinase 1/cell division cycle 2
Cdc25c	Cell division cycle 25 homolog C

Acknowledgments

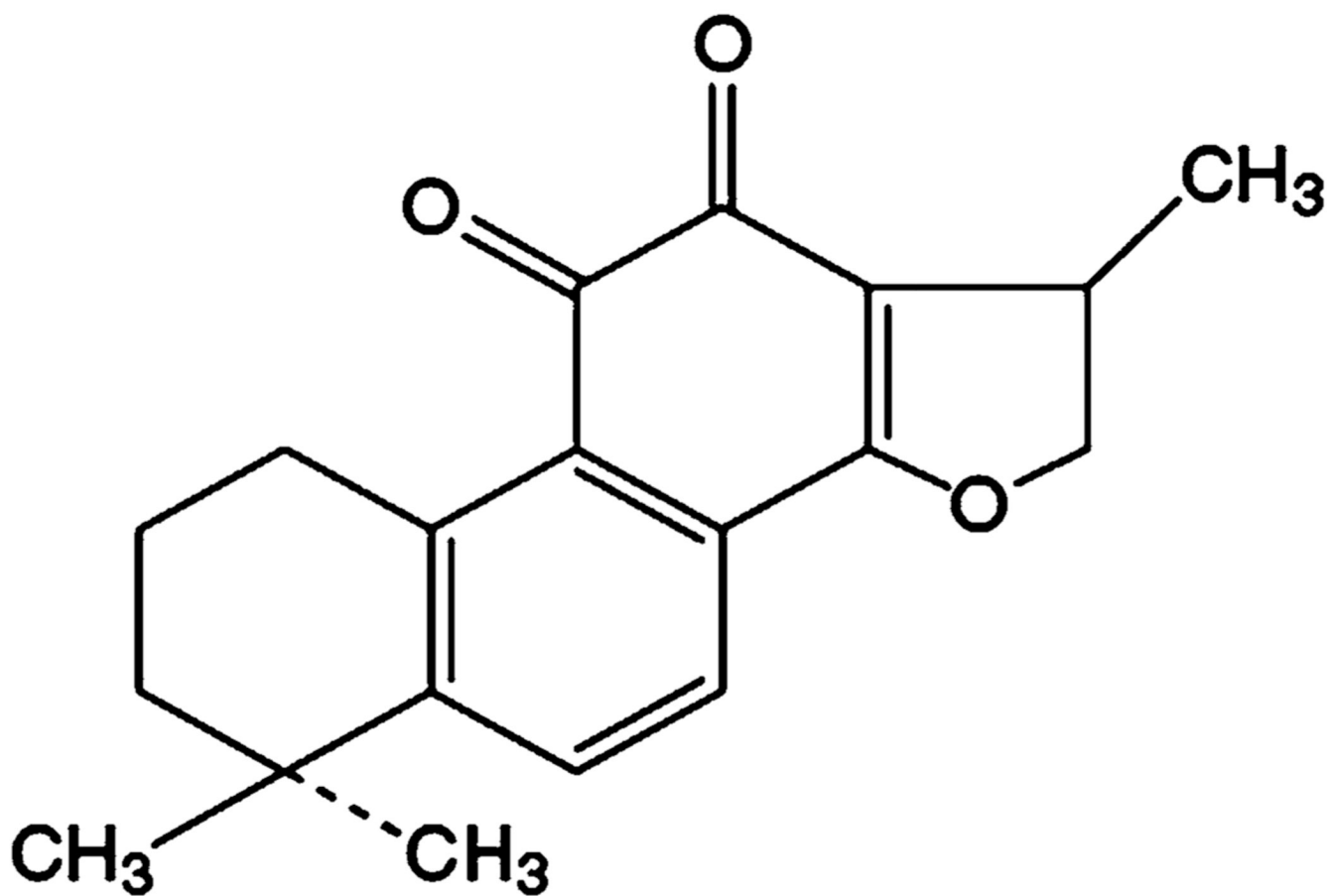
We are grateful for financial support from National Nature Science Foundation of China (Project No. 30772766), Nature Science Foundation of Jiangsu Province (Project No. BK2007239) and Educational Commission of Jiangsu Province (Project No. 09KJA360002). We also appreciate Dr. Bin Chen for the thoughtful revision.

References

1. Gray-Schopfer V, Wellbrock C, Marais R. Melanoma biology and new targeted therapy. *Nature*. 2007; 445:851–857. [PubMed: 17314971]

2. Marquette A, Bagot M, Bensussan A, Dumaz N. Recent discoveries in the genetics of melanoma and their therapeutic implications. *Arch Immunol Ther Exp (Warsz)*. 2007; 55:363–372. [PubMed: 18060370]
3. Lens M. Current clinical overview of cutaneous melanoma. *Br J Nurs*. 2008; 17:300–305. [PubMed: 18414292]
4. Kaufmann WK, Nevis KR, Qu P, Ibrahim JG, Zhou T, Zhou Y, Simpson DA, Helms-Deaton J, Cordeiro-Stone M, Moore DT, Thomas NE, Hao H, Liu Z, Shields JM, Scott GA, Sharpless NE. Defective cell cycle checkpoint functions in melanoma are associated with altered patterns of gene expression. *J Invest Dermatol*. 2008; 128:175–187. [PubMed: 17597816]
5. Fan TP, Yeh JC, Leung KW, Yue PY, Wong RN. Angiogenesis: from plants to blood vessels. *Trends Pharmacol Sci*. 2006; 27:297–309. [PubMed: 16697473]
6. Zhang F, Zheng W, Pi R, Mei Z, Bao Y, Gao J, Tang W, Chen S, Liu P. Cryptotanshinone protects primary rat cortical neurons from glutamate-induced neurotoxicity via the activation of the phosphatidylinositol 3-kinase/Akt signaling pathway. *Exp Brain Res*. 2009; 193:109–118. [PubMed: 18936923]
7. Zhou L, Zuo Z, Chow MS. Danshen: an overview of its chemistry, pharmacology, pharmacokinetics, and clinical use. *J Clin Pharmacol*. 2005; 45:1345–1359. [PubMed: 16291709]
8. Wang BE. Treatment of chronic liver diseases with traditional Chinese medicine. *J Gastroenterol Hepatol*. 2000; 15 Suppl:E67–E70. [PubMed: 10921385]
9. Yu XY, Lin SG, Chen X, Zhou ZW, Liang J, Duan W, Chowbay B, Wen JY, Chan E, Cao J, Li CG, Zhou SF. Transport of cryptotanshinone, a major active triterpenoid in *Salvia miltiorrhiza* Bunge widely used in the treatment of stroke and Alzheimer's disease, across the blood-brain barrier. *Curr Drug Metab*. 2007; 8:365–378. [PubMed: 17504224]
10. Hur JM, Shim JS, Jung HJ, Kwon HJ. Cryptotanshinone but not tanshinone IIA inhibits angiogenesis in vitro. *Exp Mol Med*. 2005; 37:133–137. [PubMed: 15886527]
11. Kang BY, Chung SW, Kim SH, Ryu SY, Kim TS. Inhibition of interleukin-12 and interferon-gamma production in immune cells by tanshinones from *Salvia miltiorrhiza*. *Immunopharmacology*. 2000; 49:355–361. [PubMed: 10996033]
12. Lee DS, Lee SH, Noh JG, Hong SD. Antibacterial activities of cryptotanshinone and dihydrotanshinone I from a medicinal herb, *Salvia miltiorrhiza* Bunge. *Biosci Biotechnol Biochem*. 1999; 63:2236–2239. [PubMed: 10664860]
13. Ren Y, Houghton PJ, Hider RC, Howes MJ. Novel diterpenoid acetylcholinesterase inhibitors from *Salvia miltiorrhiza*. *Planta Med*. 2004; 70:201–204. [PubMed: 15114495]
14. Ryu SY, Oak MH, Kim KM. Inhibition of mast cell degranulation by tanshinones from the roots of *Salvia miltiorrhiza*. *Planta Med*. 1999; 65:654–655. [PubMed: 10575380]
15. Wang AM, Sha SH, Lesniak W, Schacht J. Tanshinone (*Salviae miltiorrhizae* extract) preparations attenuate aminoglycoside-induced free radical formation in vitro and ototoxicity in vivo. *Antimicrob Agents Chemother*. 2003; 47:1836–1841. [PubMed: 12760856]
16. Nizamutdinova IT, Lee GW, Son KH, Jeon SJ, Kang SS, Kim YS, Lee JH, Seo HG, Chang KC, Kim HJ. Tanshinone I effectively induces apoptosis in estrogen receptor-positive (MCF-7) and estrogen receptor-negative (MDA-MB-231) breast cancer cells. *Int J Oncol*. 2008; 33:485–491. [PubMed: 18695877]
17. Shin DS, Kim HN, Shin KD, Yoon YJ, Kim SJ, Han DC, Kwon BM. Cryptotanshinone inhibits constitutive signal transducer and activator of transcription 3 function through blocking the dimerization in DU145 prostate cancer cells. *Cancer Res*. 2009; 69:193–202. [PubMed: 19118003]
18. Zhang W, Li D, Mehta JL. Role of AIF in human coronary artery endothelial cell apoptosis. *Am J Physiol Heart Circ Physiol*. 2004; 286:H354–H358. [PubMed: 14684364]
19. Melnikova VO, Bolshakov SV, Walker C, Ananthaswamy HN. Genomic alterations in spontaneous and carcinogen-induced murine melanoma cell lines. *Oncogene*. 2004; 23:2347–2356. [PubMed: 14743208]
20. Hartwell LH, Weinert TA. Checkpoints: controls that ensure the order of cell cycle events. *Science*. 1989; 246:629–634. [PubMed: 2683079]
21. Liu Q, Guntuku S, Cui XS, Matsuoka S, Cortez D, Tamai K, Luo G, Carattini-Rivera S, DeMayo F, Bradley A, Donehower LA, Elledge SJ. Chk1 is an essential kinase that is regulated by Atr and

- required for the G(2)/M DNA damage checkpoint. *Genes Dev.* 2000; 14:1448–1459. [PubMed: 10859164]
22. Abbas T, Dutta A. p21 in cancer: intricate networks and multiple activities. *Nat Rev Cancer.* 2009; 9:400–414. [PubMed: 19440234]
23. Rhind N, Russell P. Chk1 and Cds1: linchpins of the DNA damage and replication checkpoint pathways. *J Cell Sci.* 2000; 113(Pt 22):3889–3896. [PubMed: 11058076]
24. Bartek J, Lukas J. Chk1 and Chk2 kinases in checkpoint control and cancer. *Cancer Cell.* 2003; 3:421–429. [PubMed: 12781359]
25. Manni I, Mazzaro G, Gurtner A, Mantovani R, Haugwitz U, Krause K, Engeland K, Sacchi A, Soddu S, Piaggio G. NF-Y mediates the transcriptional inhibition of the cyclin B1, cyclin B2, and cdc25C promoters upon induced G2 arrest. *J Biol Chem.* 2001; 276:5570–5576. [PubMed: 11096075]
26. Rigel DS, Carucci JA. Malignant melanoma: prevention, early detection, and treatment in the 21st century. *CA Cancer J Clin.* 2000; 50:215–236. quiz 237–240. [PubMed: 10986965]
27. Casagrande F, Darbon JM. Effects of structurally related flavonoids on cell cycle progression of human melanoma cells: regulation of cyclin-dependent kinases CDK2 and CDK1. *Biochem Pharmacol.* 2001; 61:1205–1215. [PubMed: 11322924]
28. Ling YH, Jiang JD, Holland JF, Perez-Soler R. Arsenic trioxide produces polymerization of microtubules and mitotic arrest before apoptosis in human tumor cell lines. *Mol Pharmacol.* 2002; 62:529–538. [PubMed: 12181429]
29. Mosaddik MA. In vitro cytotoxicity of tanshinones isolated from *Salvia miltiorrhiza* Bunge against P388 lymphocytic leukemia cells. *Phytomedicine.* 2003; 10:682–685. [PubMed: 14692730]



Cryptotanshinone

Fig. 1.
Structure of Cryptotanshinone

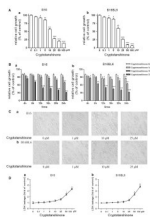


Fig. 2. Effect of Cryptotanshinone on B16 and B16BL6 melanoma cell growth. **a** The effect of Cryptotanshinone in different concentrations on B16 and B16BL6 melanoma cell growth. **b** The effect of Cryptotanshinone on B16 and B16BL6 melanoma cell growth at different time points. The cell growth was evaluated by MTT assay. The reading of control was normalized to 100%, and readings from Cryptotanshinone-treated cells were expressed as % of control (Cryptotanshinone 0 μ M). **c** The effect of Cryptotanshinone on B16 and B16BL6 melanoma cell morphology. After incubation with Cryptotanshinone for 24 h, images of the cell morphological changes were taken with an inverted microscope at a $\times 100$ magnification. **d** The cytotoxic effect of Cryptotanshinone on B16 and B16BL6 melanoma cell. After treatment with Cryptotanshinone for 24 h, culture supernatants were then collected and cell cytotoxicity was measured by LDH release assay. Values are presented as fold normalized activity relative to that of control. Data are all presented as mean \pm SEM. (* $P < 0.05$, ** $P < 0.01$, *** $P < 0.001$ vs. control). *a* For B16 melanoma cell line; *b* for B16BL6 melanoma cell line

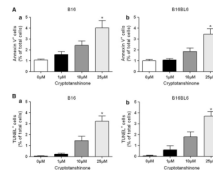


Fig. 3.

Effect of Cryptotanshinone on B16 and B16BL6 melanoma cell apoptosis in the early stage. **a** The effect of Cryptotanshinone on B16 and B16BL6 melanoma cell apoptosis in the early stage. **b** The effect of Cryptotanshinone on B16 and B16BL6 melanoma cell apoptosis in the last phase. Proliferating cells were exposed to Cryptotanshinone (0, 1, 10 and 25 μ M) for 24 h, and the apoptotic cells in the early stage were determined by Annexin V/PI using flow cytometric analysis. The Annexin V labeling index was defined as the percentage of Annexin V-positive and PI-negative cells against total cells counted. The apoptotic cells in the last phase were measured by TUNEL immunofluorescence assay. The TUNEL labeling index was defined as the percentage of TUNEL-positive cells against total cells counted. Columns, mean of triplicates; bars, \pm SEM. (* $P < 0.05$ vs. control). *a* For B16 melanoma cell line; *b* for B16BL6 melanoma cell line

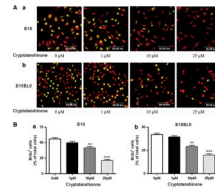


Fig. 4.

Effect of Cryptotanshinone on B16 and B16BL6 melanoma cell proliferation (DNA synthesis). Cells were treated with Cryptotanshinone (0, 1, 10 and 25 μM) for 24 h. Cells in S phase (DNA synthesis) were labeled by BrdU incorporation, assayed by immunostaining and counted by confocal microscope. The representative photographs of immunofluorescence of BrdU and Topro-3 in Cryptotanshinone-treated cells were shown in (a). The BrdU labeling index was shown in (b), which is defined as the percentage of BrdU-positive cells against total cells counted. Columns, mean of triplicates; bars, $\pm\text{SEM}$. (** $P < 0.01$, *** $P < 0.001$ versus control). *a* For B16 melanoma cell line; *b* for B16BL6 melanoma cell line

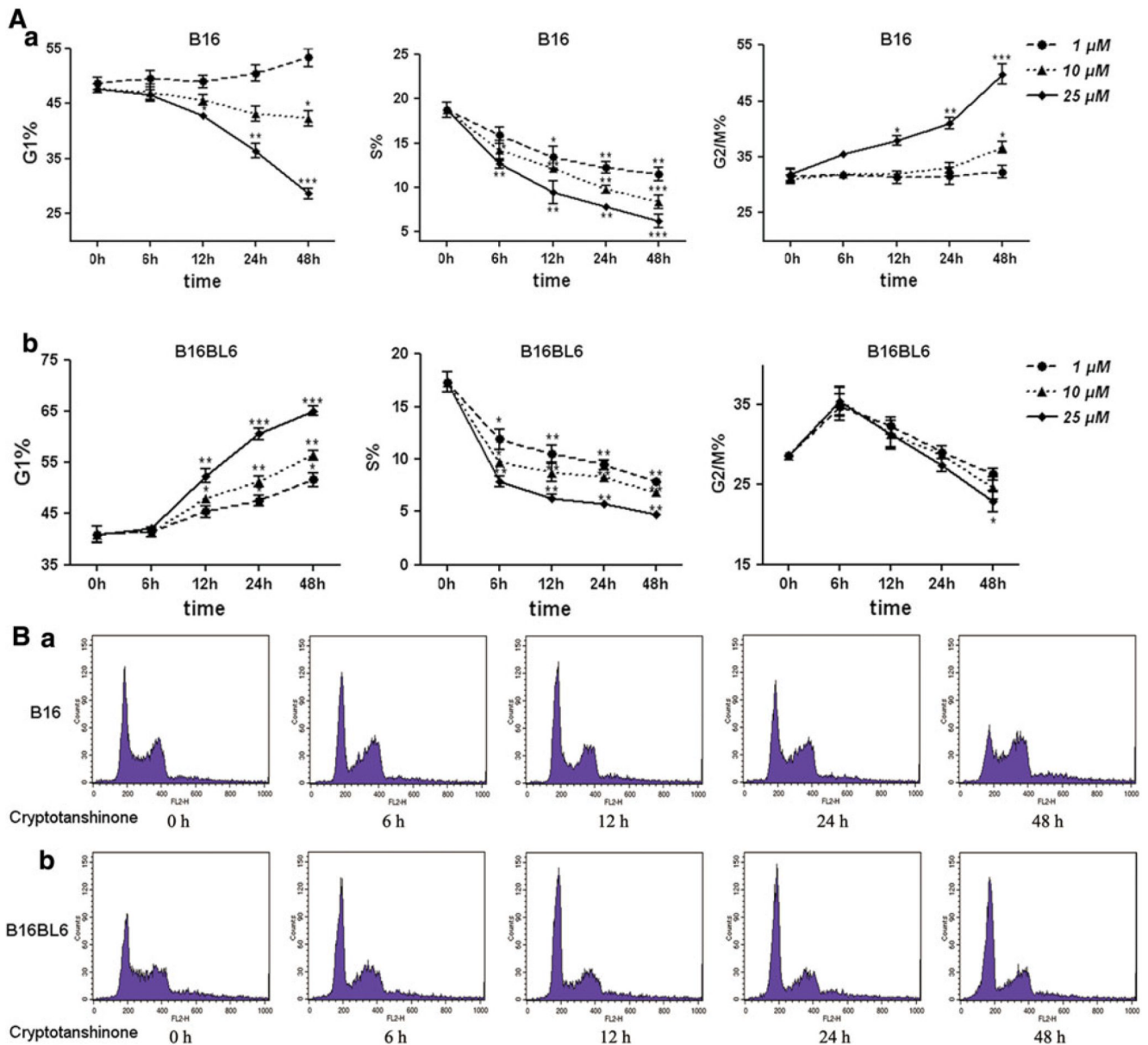


Fig. 5. Effect of Cryptotanshinone on B16 and B16BL6 melanoma cell cycle. Cells were plated at 3×10^5 cells per 60-mm dish, incubated for 12 h, transferred to fresh medium and treated with different concentrations of Cryptotanshinone (0, 1, 10 and 25 μM) for 0, 6, 12, 24 and 48 h. After incubation for different periods of time, cells were collected, stained and analyzed by flow cytometry for cell distribution at each phase of the cell cycle. **a** Calculation of cell cycle distribution using CellQuest analysis software. Data are the means \pm SEM. obtained from a triplicate of each experiment. * $P < 0.1$, ** $P < 0.01$, *** $P < 0.001$ versus control (Cryptotanshinone 0 μM , 0 h). **b** The typical pattern of DNA content of cell cycle distribution in Cryptotanshinone (25 μM)-treated cells at different time points. *a* For B16 melanoma cell line; *b* for B16BL6 melanoma cell line

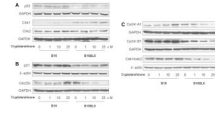


Fig. 6. Effect of Cryptotanshinone on the expression of cell cycle-associated proteins in B16 and B16BL6 melanoma cells. Cells were treated with Cryptotanshinone (0, 1, 10 and 25 μ M) for 24 h. Whole-cell extracts were analyzed by western blotting using the indicated antibody. β -actin or GAPDH was used as an internal control to monitor equal protein loading. **a** The effect of Cryptotanshinone on the expression of p53, Chk1 and Chk2 in B16 and B16BL6 melanoma cells. **b** The effect of Cryptotanshinone on the expression of p21 and Cdc25c in B16 and B16BL6 melanoma cells. **c** The effect of Cryptotanshinone on the expression of Cyclin A1, Cyclin B1 and Cdk1/cdc2 in B16 and B16BL6 melanoma cells